Supplementary Information

A covalent organic framework membrane with electron-enriched channels for modulating hydrated zinc ion transport

Jiaxin Liu, [a] *Yunyi Zhang,* [a] *Zhanyang Dong,* [a] *Hongli Yang,* [a] *Shengyang Zhou,* [a] [*]*Zhong-Ming Li* [b]

[a] College of Materials Science and Engineering, College of Polymer Science and Engineering, State Key Laboratory of Advanced Polymer Materials, Sichuan University, Chengdu 610065, China. [*]E-mail: shengyang.zhou@scu.edu.cn

[b] Institute of Cardiovascular Surgery, West China Hospital, Sichuan University, Chengdu 610041, China.

Experimental Section

Materials.

Zinc sulfate heptahydrate ($ZnSO_4 \cdot 7H_2O$, analytical reagent grade) was purchased from Aladdin. Zinc foil with a thickness of 50 μm, copper foil with a thickness of 50 μm, and glass fiber separators were obtained from Olegeeino. Bacterial nanocellulose aqueous dispersion (BNC, 1 wt%) was supplied by Cellubio. 2,4,6-Triformylphloroglucinol (TFP), tris(4-aminophenyl)amine (TAPA), and acetic acid (AcOH) were purchased from Aladdin. The V_2O_5 cathodes were provided by Future (Jilin) Materials Tech. Co., Ltd. All chemicals and materials were used as received without further purification unless otherwise specified. Ultrapure water used throughout the experiments was produced using an ultrapure water purification system supplied by Shanghai Lichen Instrument Technology Co., Ltd.

Synthesis of TAPA-TFP COF.

2,4,6-Triformylphloroglucinol (TFP, 129 mg, 0.6 mmol) was added to a 20 mL glass vial, followed by the addition of 3M aqueous acetic acid solution (AcOH, 2 mL). The mixture was magnetically stirred at 400 rpm for 30 min at room temperature to obtain a homogeneous solution. Separately, tris(4-aminophenyl)amine (TAPA, 269 mg, 0.9 mmol) was dissolved in ultrapure water (4 mL) to form an amine solution. The TAPA solution was then added dropwise to the TFP solution under continuous stirring at a controlled rate of approximately 1 mL min^{-1}. After the addition was completed, the vial was sealed and the reaction mixture was stirred at room temperature for 24 h. The resulting solid product was collected by centrifugation at 8000 rpm for 10 min, followed

by washing with acetone three times to remove residual monomers and acetic acid. Finally, the obtained precipitate was redispersed in ultrapure water and sonicated for 10 min to form a uniform COF slurry for subsequent membrane preparation. The chemical reaction involved in the formation of TAPA-TFP COF is illustrated in Figure S1.

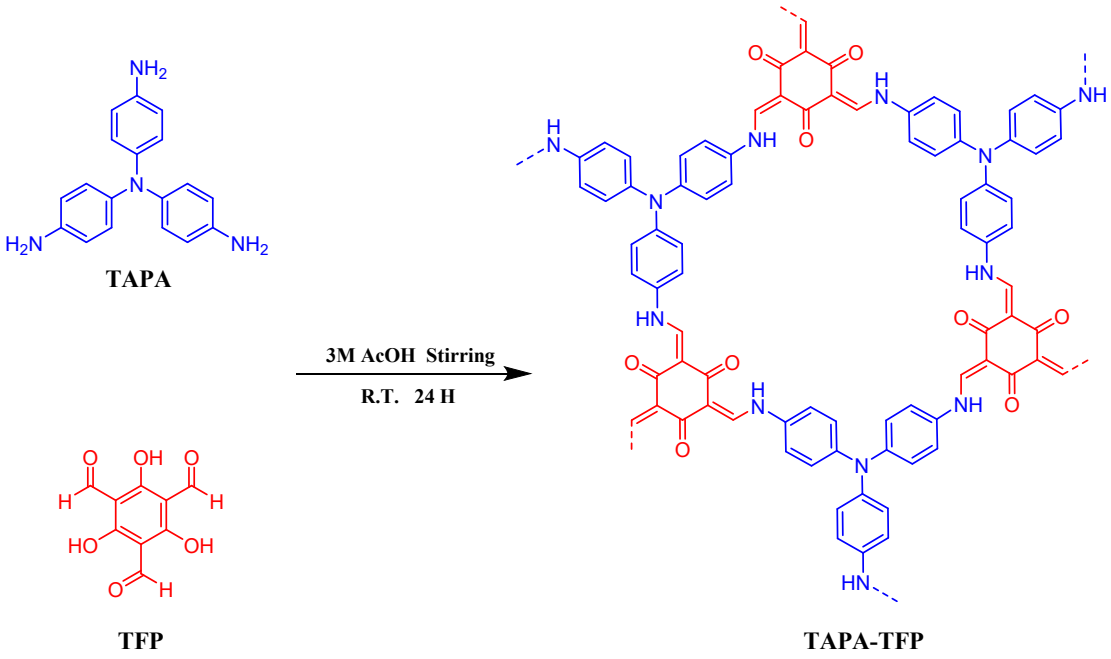

Figure S1. Synthesis of TAPA-TFP COF.

Preparation of TAPA-TFP COF membranes.

The as-prepared TAPA-TFP COF slurry (5 mL, 50 mg mL^{-1}) was added to bacterial nanocellulose aqueous dispersion (BNC, 40 mL, 2.5 mg mL^{-1}). The mixture was sonicated at room temperature for 10 min to achieve a homogeneous dispersion of COF particles within the BNC network. To improve the uniformity of the membrane, the resulting suspension was sequentially poured onto a vacuum filtration setup in three equal portions of 15 mL each. Each portion was vacuum-filtered at −0.08 MPa until no

visible liquid remained on the membrane surface, yielding a uniform wet membrane. The wet membrane, together with the filter substrate, was carefully sandwiched between two stainless-steel plates and dried in a vacuum oven at 60 °C for 12 h. After drying, the composite membrane was peeled from the filter substrate and punched into circular discs with a diameter of 16 mm for subsequent battery assembly.

Materials Characterization.

X-ray diffraction (XRD) patterns were recorded on a DX-2700B X-ray diffractometer (Haoyuan Instrument) using Cu Kα radiation. Wide-angle X-ray scattering (WAXS) patterns were acquired on beamline 16B of the Shanghai Synchrotron Radiation Facility (Shanghai, China). Transmission electron microscopy (TEM) images were obtained with an FEI Tecnai G2 F20 S-TWIN microscope. Scanning electron microscopy (SEM) observations were carried out on a Nova NanoSEM 450 instrument (FEI). Nitrogen adsorption–desorption measurements were performed using an Ankersmid Belsorp-Max analyzer to evaluate the pore characteristics. The mechanical properties of the separators were measured using a universal testing machine (INSTRON 5967), while their wettability was assessed by contact angle measurements on a Krüss DSA30S instrument. Fourier transform infrared (FTIR) spectra were collected using a Thermo Scientific Nicolet 6700 spectrometer.

Electrochemical Measurements.

Commercial Zn foil and Cu foil with a thickness of 50 μm were punched into circular discs with a diameter of 12 mm. CR2032 coin-type cells were assembled at room

temperature using 100 μL of 2 M $ZnSO_4$ aqueous electrolyte. Zn||Zn symmetric cells and Zn||Cu asymmetric cells were used to evaluate the Zn plating/stripping behavior and interfacial stability. Zn||V_2O_5 full cells were assembled under the same conditions using V_2O_5 cathodes with an active material loading of 1 mg cm^{-2}. The cycling voltage window of the Zn||V_2O_5 full cells was set between 0.2 and 1.6 V. Electrochemical measurements, including cyclic voltammetry (CV), chronoamperometry (CA), electrochemical impedance spectroscopy (EIS), Tafel polarization, and chronopotentiometry (CP), were performed on an electrochemical workstation (CHI660E, Chen Hua, China). EIS measurements were conducted over a frequency range from 0.01 Hz to 10^5 Hz. Tafel polarization curves were recorded from −0.2 to 0.2 V at a scan rate of 1 mV s^{-1}. CV measurements of Zn||Cu cells were carried out between −0.3 and 0.6 V at a scan rate of 1 mV s^{-1}. Galvanostatic charge/discharge tests were conducted using a Neware battery testing system (CT-4008T).

Ionic Conductivity Measurements.

The ionic conductivities (σ) of the separators were measured using stainless-steel blocking cells. The separator was soaked with electrolyte and sandwiched between two stainless-steel electrodes, followed by EIS measurement. The ionic conductivity was calculated according to the following equation:

$$\sigma = \frac{L}{RS}$$

where L is the thickness of the separator, R is the bulk resistance obtained from the EIS spectrum, and S is the effective contact area between the separator and the stainless-steel electrode.

Zn^{2+} Transference Number Measurements.

The Zn^{2+} transference numbers ($t_{Zn^{2+}}$) of different separators were determined using Zn||Zn symmetric cells by combining chronoamperometry (CA) and electrochemical impedance spectroscopy (EIS) measurements. A constant polarization voltage of 50 mV was applied to the cells, and EIS spectra were collected before and after polarization. The $t_{Zn^{2+}}$ values were calculated according to the following equation:

$$t_{Zn^{2+}} = \frac{I_S(\Delta V - I_0 R_0)}{I_0(\Delta V - I_S R_S)}$$

where ΔV is the applied polarization voltage of 50 mV; I_0 and I_s represent the initial current and steady-state current obtained from the CA curves, respectively; R_0 and R_s are the interfacial resistances before and after polarization, respectively, determined from the EIS spectra.

Measurement of Zn^{2+} Diffusion Coefficient.

The Zn^{2+} diffusion coefficient was evaluated using Zn||Cu cells based on cyclic voltammetry (CV) measurements at different scan rates. CV curves were recorded within the same voltage window at various scan rates. The Zn^{2+} diffusion coefficient was calculated according to the Randles–Sevcik equation:

$$I_p = 0.4463nFAC_{Zn^{2+}} v^{1/2} \left(\frac{nFD_{Zn^{2+}}}{RT}\right)^{1/2}$$

where I_p is the peak current, n is the number of electrons involved in the electrode reaction, F is the Faraday constant, A is the contact area, $C_{Zn^{2+}}$ is the concentration of Zn^{2+} in the electrolyte, V is the scan rate, $D_{Zn^{2+}}$ is the Zn^{2+} diffusion coefficient, R is

the gas constant, and T is the absolute temperature.

Adsorption energy calculation.

Adsorption energies were calculated using density functional theory (DFT) with the ORCA program. Simplified molecular models were constructed to represent the local coordination environment of the TAPA-TFP framework. The H_2O–COF, Zn^{2+}–H_2O, and Zn^{2+}–COF complexes were fully optimized at the PBE0-D3/def2-SVP level with Grimme's D3 dispersion correction. Solvent effects were considered using the CPCM model with water as the solvent. Single-point energy calculations were then performed at the ωB97M-V/def2-TZVP level to obtain more accurate electronic energies, with effective core potentials applied to Zn atoms. The adsorption energy (ΔE) was calculated as follows:

$$\Delta E = E_{complex} - E_{adsorbate} - E_{substrate}$$

where $E_{complex}$ is the total energy of the optimized complex, $E_{adsorbate}$ is the energy of H_2O or Zn^{2+}, and $E_{substrate}$ is the energy of H_2O or the TAPA-TFP COF fragment, calculated under the same conditions. A more negative ΔE value indicates a stronger interaction. The simplified TAPA-TFP fragment was used to retain the key coordination sites of the COF framework.

Supplementary Results

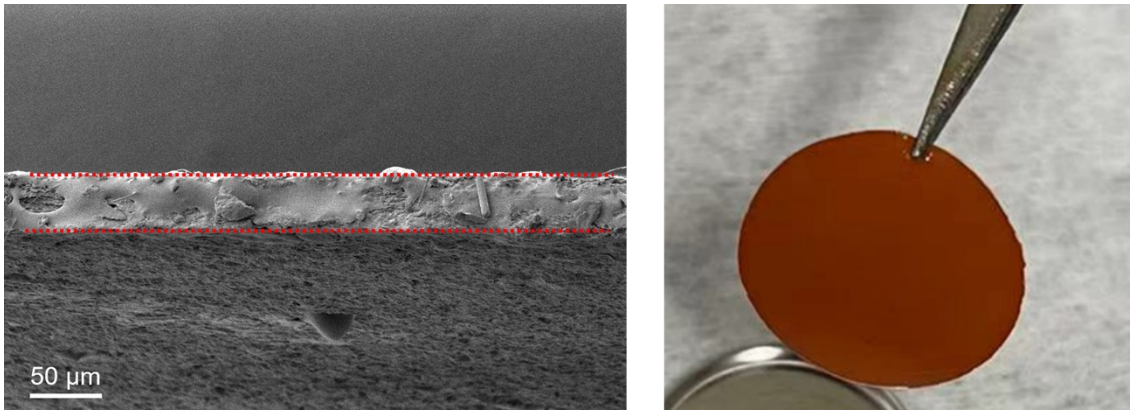

Figure S2. Cross-sectional SEM image and optical photograph of the TAPA-TFP membrane.

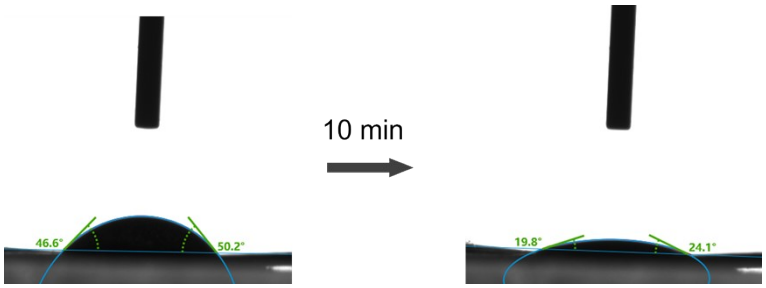

Figure S3. Electrolyte contact angle measurement of the TAPA-TFP membrane.

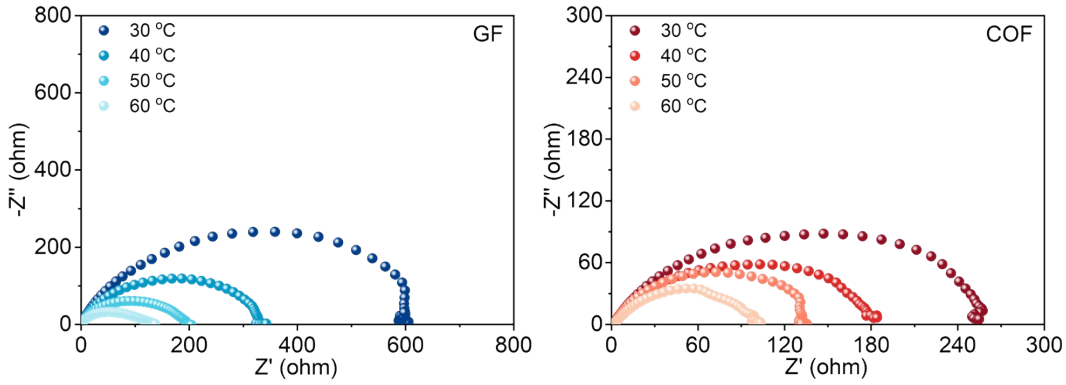

Figure S4. EIS profiles of GF and TAPA-TFP COF membranes in 2 M $ZnSO_4$ electrolyte.

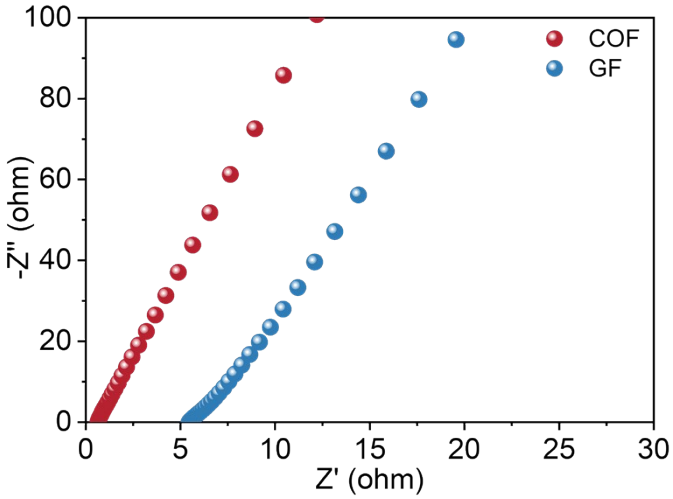

Figure S5. EIS profiles of GF and TAPA-TFP COF membrane.

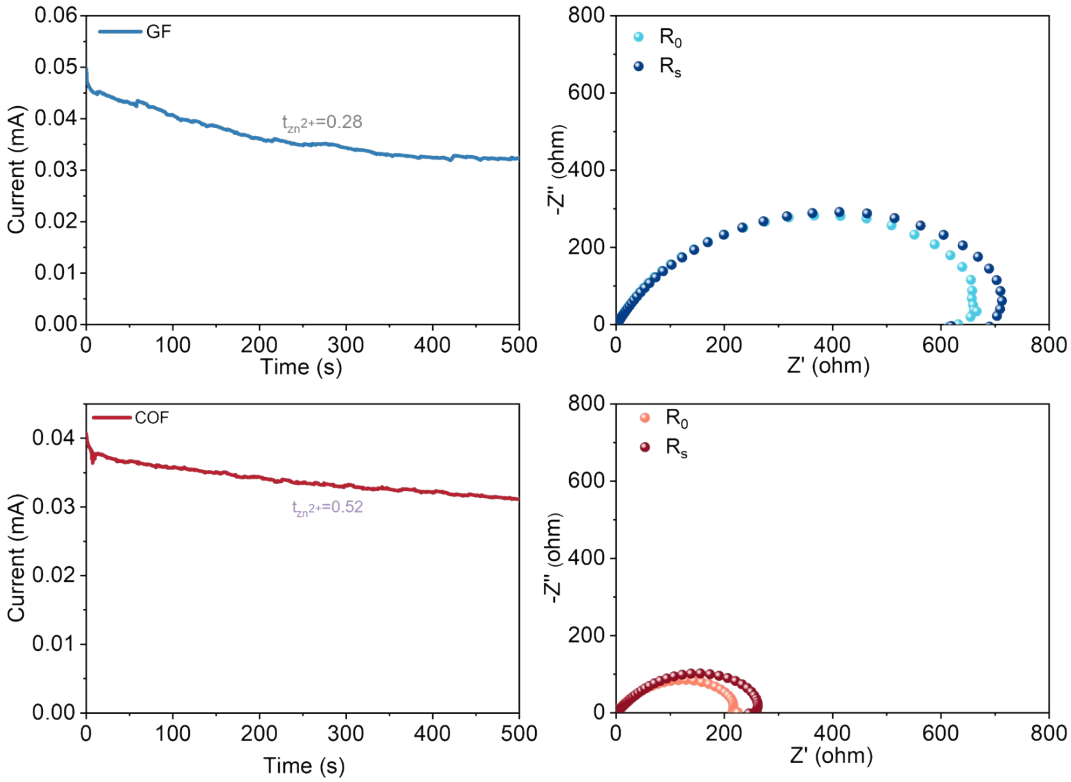

Figure S6. CA curves and EIS spectra before and after polarization for determining the Zn^{2+} transference numbers of GF and TAPA-TFP COF membranes.

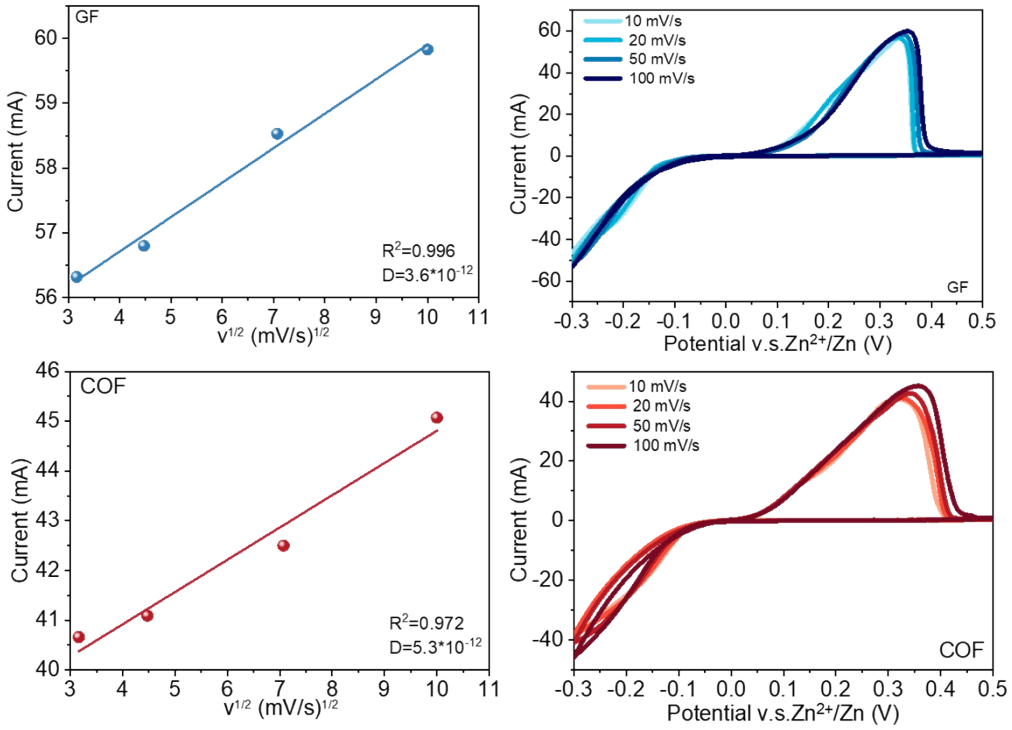

Figure S7. Scan-rate-dependent CV curves and corresponding fitting results for calculating Zn^{2+} diffusion coefficients in GF- and TAPA-TFP COF based Zn||Cu cells.

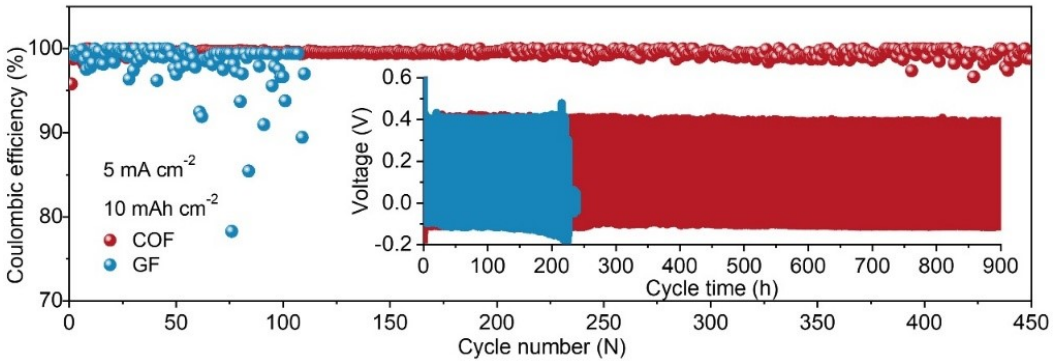

Figure S8. Coulombic efficiency during cycling of Zn-Cu cells at a large current density of 5mA cm^{-2} (inset shows the charge-discharge profile).

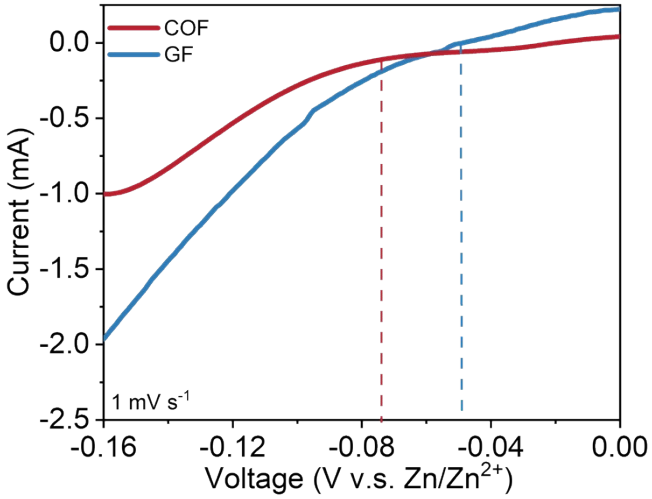

Figure S9. Linear sweep voltammetry curves of GF and TAPA-TFP COF cells.

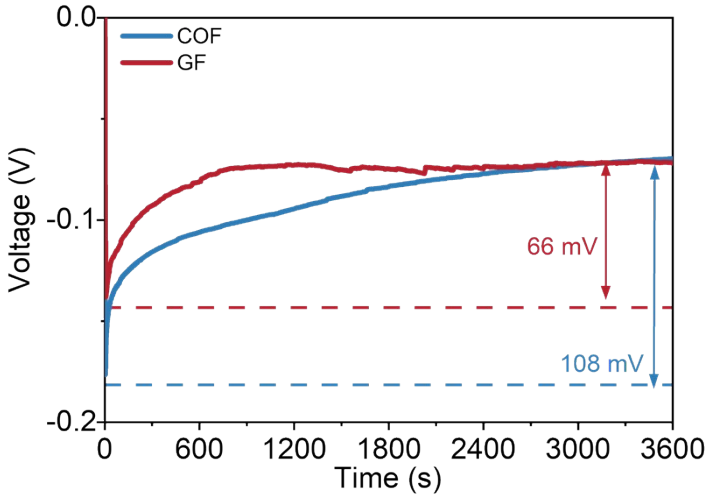

Figure S10. Zn nucleation overpotential profiles of GF and TAPA-TFP COF cells.

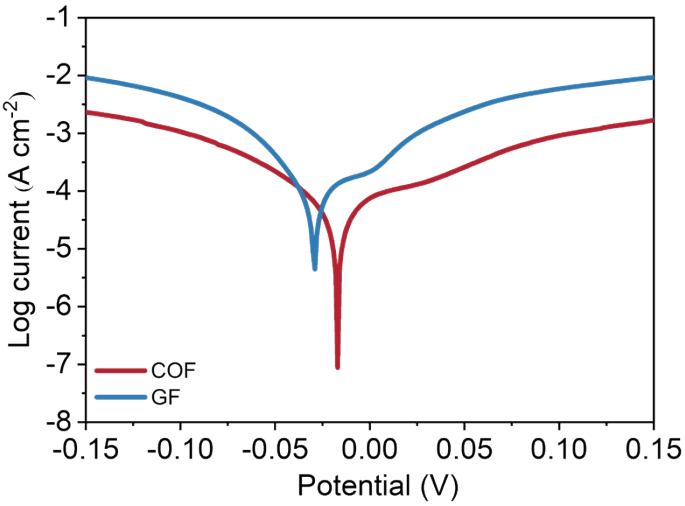

Figure S11. Tafel curves of Zn//Zn cell.

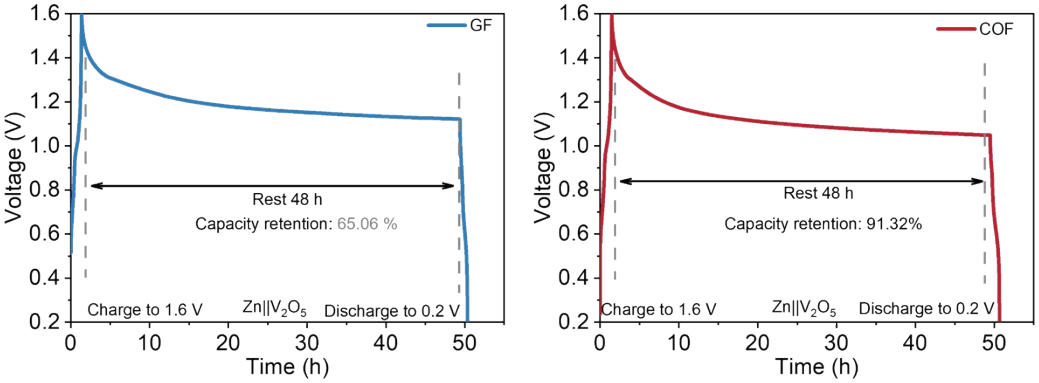

Figure S12. Self-discharge comparison of Zn||V_2O_5 full cells.